Int J Appl Earth Obs Geoinformation 75 (2019) 118–129

Contents lists available at ScienceDirect

Int J Appl Earth Obs Geoinformation

journal homepage: www.elsevier.com/locate/jag

Mapping irrigated agriculture in complex landscapes using SPOT6 imagery and object-based image analysis – A case study in the Central Rift Valley, Ethiopia –

M.F.A. Vogels*, S.M. de Jong, G. Sterk, E.A. Addink

Utrecht University, Department of Physical Geography, PO box 80115, 3508 TC Utrecht, The Netherlands

ARTICLE INFO

Keywords:
Smallholder irrigation
GEOBIA
Field-level analysis
Agriculture
Data-poor regions
Ethiopia
Central Rift Valley

ABSTRACT

Irrigation infrastructure development for smallholder farmers in developing countries increasingly gains attention in the light of domestic food security and poverty alleviation. However, these complex landscapes with small cultivated plots pose a challenge with regard to mapping and monitoring irrigated agriculture. This study presents an object-based approach to map irrigated agriculture in an area in the Central Rift Valley in Ethiopia using SPOT6 imagery. The study is a proof-of-concept that the use of shape, texture, neighbour and location information next to spectral information is beneficial for the classification of irrigated agriculture. The underlying assumption is that the application of irrigation has a positive effect on crop growth throughout the field, following the field's borders, which is detectable in an object-based approach. The type of agricultural system was also mapped, distinguishing smallholder farming and modern large-scale agriculture. Irrigated agriculture was mapped with an overall accuracy of 94% and a kappa coefficient of 0.85. Producer's and user's accuracies were on average 90.6% and 84.2% respectively. The distinction between smallholder farming and large-scale agriculture was identified with an overall accuracy of 95% and a kappa coefficient of 0.88. The classifications were performed at the field level, since the segmentation was able to adequately delineate individual fields. The additional use of object features proved essential for the identification of cropland plots, irrigation period and type of agricultural system. This method is independent of expert knowledge on crop phenology and absolute spectral values. The proposed method is useful for the assessment of spatio-temporal dynamics of irrigated (smallholder) agriculture in complex landscapes and yields a basis for land and water managers on agricultural water use.

1. Introduction

Agriculture is currently responsible for about 70% of world's freshwater withdrawals (WWAP, 2012). Agricultural water consumption will continue to rise as global population growth projections reveal an increase in food demand of 70% by 2050 (Bruinsma, 2009). Irrigated crop yield is approximately 2.7 times higher than rainfed crop yield, hence irrigation will play an increasingly important role in food production and food security (WWAP, 2012). Global irrigation-equipped area increased from 170 million ha in 1970 to 304 million ha in 2008 (Bruinsma, 2009). For the developing world opportunities are not fully exploited, e.g. only about 20% of Africa's total irrigation potential is currently utilized (WWAP, 2012).

Irrigation is the controlled application of water to land to enable or to enhance crop growth in the absence of sufficient or timely rainfall (USGS, 2016a). Irrigation results in a different crop phenology as compared to purely rainfed agriculture leading to different spatio-temporal vegetation distributions (Thenkabail et al., 2005). In the landscape, irrigated agriculture can be recognized by more active and more productive vegetation than can be supported by the direct surroundings. Especially in (semi-)arid regions, at locations where the same crops are cultivated with and without irrigation, an irrigated crop can readily be distinguished from non-irrigated crops by pronounced differences in greenness and biomass (Thiruvengadachari, 1981). Besides, a general landscape characteristic of agriculture is that crops are distributed in fields and that crop management (irrigation) is applied to entire fields (field level). Irrigated fields are often part of a larger irrigated area (irrigation scheme) and not scattered across the landscape. Furthermore, the irrigated areas are located in the vicinity of water (resources) such as rivers, pumps, ponds, reservoirs or lakes.

* Corresponding author.
E-mail address: m.f.a.vogels@uu.nl (M.F.A. Vogels).

https://doi.org/10.1016/j.jag.2018.07.019
Received 28 May 2018; Received in revised form 20 July 2018; Accepted 21 July 2018
Available online 02 November 2018

Characteristic for agriculture in developing countries are the highly complex landscapes (Ozdogan et al., 2010). The small agricultural fields are dominantly cultivated by smallholder farmers, i.e. the traditional farming system producing crops mainly for domestic purposes (Abate et al., 2000). Often multiple crop types are grown either by intercropping or by mixed cropping. Planting schedules fluctuate with the seasons and often follow the timing of the rainy seasons. Smallholder irrigated agriculture mainly uses surface water as groundwater pumps are expensive. Irrigation water is applied to crops mostly by furrow or flood irrigation in the absence of mechanical techniques (USGS, 2016b).

International development policy focuses on smallholder agriculture to improve food security at the domestic level by adopting smallholder irrigation development as the main strategy (IAC, 2004; World Bank, 2008; Tschirley, 2011; Burney and Naylor, 2012). Accurate information on the extent of irrigation is essential for the assessment of the impact of irrigation on catchment hydrology (Beilicci and Beilicci, 2016), for the management of water resources for food security (Vorosmarty and Sahagain, 2000; Droogers and Aerts, 2005) and also for the assessment and evaluation of national investments in irrigation infrastructure (FAO, 2011). Efforts to identify smallholder irrigation (potential) in the developing world (e.g. You et al., 2011; Xie et al., 2014) are often too coarse for the complex agricultural landscape (Beekman et al., 2014). Previous irrigation studies mainly focus on areas with established irrigation infrastructure, thereby excluding irrigation from other sources such as river and stream diversions or farm dams, characteristic for the developing world (Abuzar et al., 2015). Consequently, the area under smallholder irrigation is often underestimated (Beekman et al., 2014).

Over the last decades, remote sensing has developed as an advanced tool in monitoring irrigated lands for a variety of climatic settings (Ozdogan et al., 2010). Single-date imagery acquired during the peak of the growing season (semi-arid regions) can hold sufficient information for the classification of irrigated lands (Thiruvengadachari, 1981), although multi-temporal imagery is preferred as it covers the different phenology stages of the crops (Thenkabail et al., 2005; Ozdogan et al., 2010). In many irrigation assessment studies the Normalized Difference Vegetation Index (NDVI) is used to describe vegetation phenology, and expert knowledge is used to identify irrigated croplands (e.g. Ambika et al., 2016; Siddiqui et al., 2016; Meier et al., 2018). Hence, irrigation-mapping methods are often site-specific and not easily transferable to other regions and climates (Ozdogan et al., 2010). In complex landscapes with multiple irrigation periods and multiple crop types with different planting schedules, the relation between NDVI and irrigation is not straightforward (Ozdogan et al., 2010). The lack of accessible data further complicates the identification of irrigated agriculture in developing countries.

Land-use and land-cover (LULC) information (including irrigated agriculture) is traditionally derived using pixel-based image analysis (PBIA). For smallholder agriculture very-high-resolution (VHR) imagery offers the ideal resolution, but PBIA is less suitable for this resolution as the within-class spectral variability is high and spectral confusion common (Blaschke et al., 2014). A suitable approach for VHR imagery is Geographic Object-Based Image Analysis (GEOBIA). It uses object information on colour, tone, texture, pattern, shape, shadow, context and size (i.e. structural parameters) to classify the images and is superior to a PBIA approach using only spectral information (Blaschke et al., 2014). The use of objects is promising for irrigation mapping in data-poor complex landscapes (Ozdogan et al., 2010). Generally, the application of irrigation is at the field level and has a positive effect on the crop throughout the field following the field's borders. Therefore, the additional use of structural parameters in a GEOBIA approach adds information for the discrimination of irrigated agriculture compared to a purely spectral PBIA workflow. GEOBIA has been applied for smallholder cropland mapping (Wickama et al., 2015; Lebourgeois et al., 2017) and to map the spatial distribution of crops within irrigation systems (Conrad et al., 2010; Peña et al., 2014). However, GEOBIA applications for the purpose of mapping irrigated agriculture itself, i.e. to map the distribution of fields with apparent access to irrigation infrastructure are not reported in literature.

This study focuses on the proof-of-concept of mapping irrigated agriculture at the field level in a complex landscape in Ethiopia using a GEOBIA approach. The case-study area encompasses both traditional smallholder agriculture as well as a modern large-scale irrigation scheme. For this reason, also a GEOBIA mapping approach was conducted to discriminate between these two types of agricultural systems. GEOBIA is thought to be an appropriate approach as spectral properties of vegetation are not unique for different (management) types and scales of the agricultural system, and additional information on structural parameters is required. The main objectives of this study were: (1) to evaluate an object-based field-level approach to map the spatio-temporal distribution of irrigated agriculture, (2) to evaluate GEOBIA for the discrimination of traditional smallholder and modern large-scale agriculture.

2. Study site, data and methods

2.1. Data collection and preparation

2.1.1. Site description

The study area (669 km^2) is located in the Awash River basin, Rift Valley Ethiopia, 130 km east of the capital Addis Ababa (Fig. 1). The area experiences a semi-arid climate with a mean annual rainfall of 543 mm, of which on average 70% is lost by evapotranspiration (Taddese et al., 2010). There are two distinct seasons: (1) the wet season running from May to August, and (2) the dry season, in which irrigation is predominantly applied, starting in September/October and ending with the first rains in March. Irrigation developments in Ethiopia mostly occur in the Awash River basin, which serves more than five million farmers (Dejen, 2014). This study covered two irrigation schemes (Fig. 1): (1) the Metahara irrigation scheme, a modern large-scale agricultural system with a field size in the order of 10-15 ha, which was started in 1965 by the Dutch company Handels Vereniging Amsterdam and currently encompasses 11,500 ha of sugarcane, and (2) the Golgota irrigation scheme, which has a size of 600 ha and is managed by the community serving smallholder farmers (Dejen, 2014). The water source for both irrigation schemes is the Awash River. Average landholder size is 1.2 ha per farmer in the Golgota scheme, and furrow irrigation, i.e. leading water by gravity through parallel channels along the field length, is most commonly practiced here. The Metahara scheme consists of a network of earthen open canals where water is diverted from two inlets from the Awash River and distributed via secondary and tertiary channels. The major crops in the Golgota scheme are onion, tomato, maize and cabbage. The length of the cropping cycles for the crops in the study area is between 75 days and 720 days (FAO, 2010).

2.1.2. SPOT6 imagery

Three SPOT6 images were obtained for the dry season of 2013–2014: 8 November 2013 (November or Nov), 4 December 2013 (December or Dec) and 1 February 2014 (February or Feb). These images were selected based on availability in the SPOT database. SPOT6 imagery has a spatial resolution of 6 m (pan-band 1.5 m) and has four spectral bands, namely blue (450-520 nm), green (530-590 nm), red (625-695 nm) and near-infrared (NIR) (760-890 nm). These images were pansharpened using the Gram-Smith pansharpening algorithm (cubic convolution), which was followed by a conversion to Top-Of-Atmosphere reflectance. The NDVI was calculated for each of the three images. The focus of this study was to capture crop changes at the field level, i.e. to delineate similarities in spatio-temporal spectral behaviour associated with the application of irrigation. For this purpose two NDVI change maps were derived by subtracting the NDVI values of the image acquisition moment from the values in the next moment; NDVI December-November (period 1 or p1) and NDVI February–December (period 2 or p2).

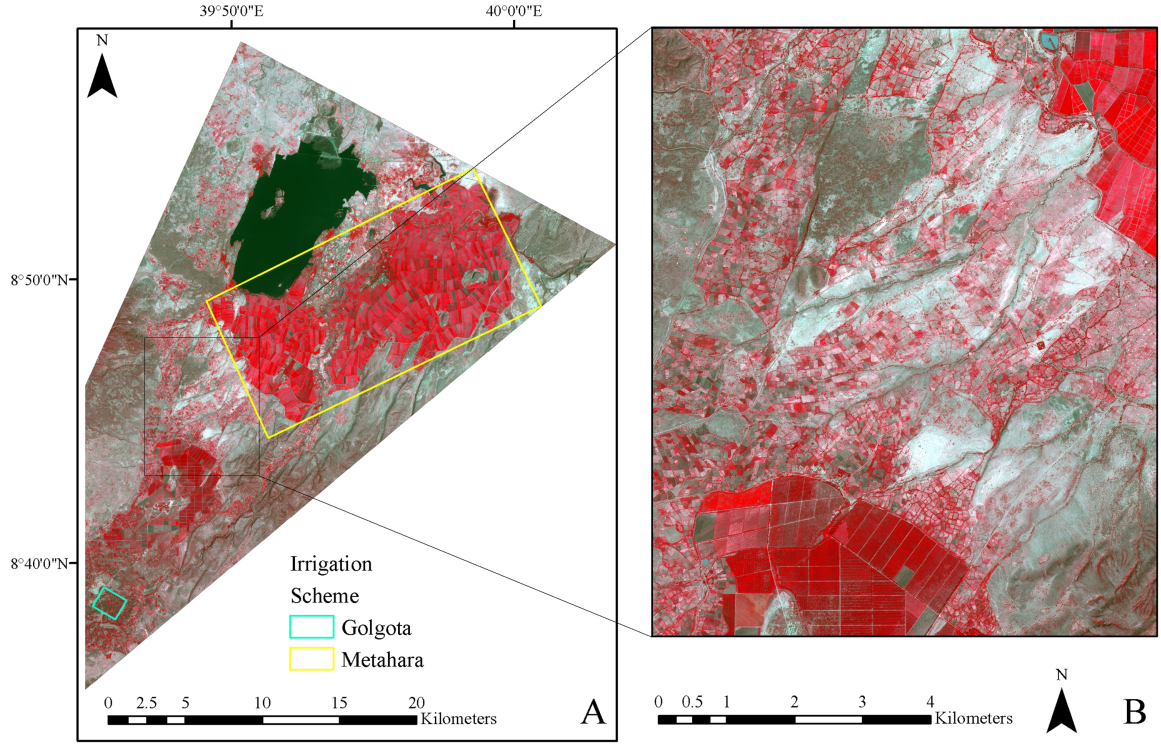

Fig. 1. A: Study area outline showing the Metahara irrigation scheme in the north-east and the Golgota irrigation scheme in the south-west on a SPOT6 image (RGB: NIR, red, green). B: Subset of the study area (RGB: NIR, red, green) highlighting the difference between modern large-scale agriculture (corners north-east and south-west) and traditional smallholder agriculture in the center of the image.

2.2. Image segmentation

An essential step in the GEOBIA approach is a successful image segmentation representing the desired scene objects, which are in this study the individual fields (Fig. 2). The segmentation is driven by a heterogeneity threshold (scale parameter), which is composed of a spectral and a shape component and can be determined by the user (Benz et al., 2004). This study assumed that generally the application of irrigation is at the field level and has a positive effect on the crop throughout the field. Therefore, objects are created on the basis of similarities in vegetation behaviour (NDVI change), and the segmentation involved a change-based grouping of pixels dominantly driven by the two NDVI-change maps. The three static NDVI maps (Nov, Dec, Feb) were added to the segmentation (lower weight: 25% each), which is desired to obtain an adequate delineation of all individual fields as it can occur that some fields show no change. Multi-resolution segmentation (Baatz and Schäpe, 2000) followed by a spectral-difference merge was applied to obtain objects of different sizes, i.e. modern large-scale agricultural fields and traditional smallholder agricultural plots. This segmentation was executed in eCognition® Developer (Trimble, 2017) and the parameters were visually optimized with a focus on the smallholder agricultural fields. For the multi-resolution segmentation a heterogeneity threshold of 150, a shape of 0.9, and a compactness of 0.5 was used. This was followed by a spectral difference merge where the maximum spectral difference was set at 50.

2.3. Image classification

2.3.1. Training and validation data

Visual interpretation of imagery is by far the most accurate, but also the most time-consuming approach as compared to (semi-)automated classification algorithms (Ozdogan et al., 2010). Especially for very high-resolution (VHR) imagery it is appropriate to perform a visual validation of the classification result (Blaschke et al., 2014). In this study 3000 objects were randomly selected to create a training and validation set for the classification. These objects were thematically labeled by visual interpretation as: (1) cropland irrigated in period 1 and period 2 (447 objects), (2) cropland irrigated in period 1 (189 objects), (3) cropland irrigated in period 2 (189 objects), (4) non-irrigated cropland (320 objects), (5) other LULC (1491 objects). Cropland irrigated in period 1 and/or period 2 is here defined as an observed greening of the vegetation or the presence of a consistent high vegetation cover in these periods. Duration and timing of irrigation is unknown. The cropland objects were also labeled for type of agriculture, either traditional smallholder (596 objects) or modern large-scale agriculture (549 objects). The material for this visual interpretation comprised the three pan-sharpened SPOT6 satellite images in a false-colour setting highlighting vegetation, a layer stack of the three NDVI images, which showed the temporal behaviour of vegetation, and ancillary information from World Imagery (ArcMap) and Google Maps (ESRI, 2017; Google Maps, 2017). If multiple land-cover types were present, the dominant land cover (> 75%) was chosen to label the object. Three situations could occur to discard an object: either its class could not be identified (0.3%), it did not contain a dominant land cover (8.9%) or land cover was obscured by clouds (2.9%). LULC and irrigation period could be identified for 88% of the objects. The final dataset comprised 2636 objects, which were equally split per class in training (1316 objects) and validation (1320 objects).

2.3.2. Object-based image classification using the Random-Forest classifier

For the classification, 17 spectral variables, 8 shape variables, 22 texture variables, 8 neighbour variables and 2 location variables (x and y coordinate) were derived for each object (57 variables in total, Appendix A). The Random Forest algorithm was used for the classification, which is a statistical classifier (Breiman, 2001). This machine learning algorithm uses multiple decision trees to create a statistical model based on sample training information and uses a majority vote for the prediction (Liaw and Wiener, 2002). Random Forests are

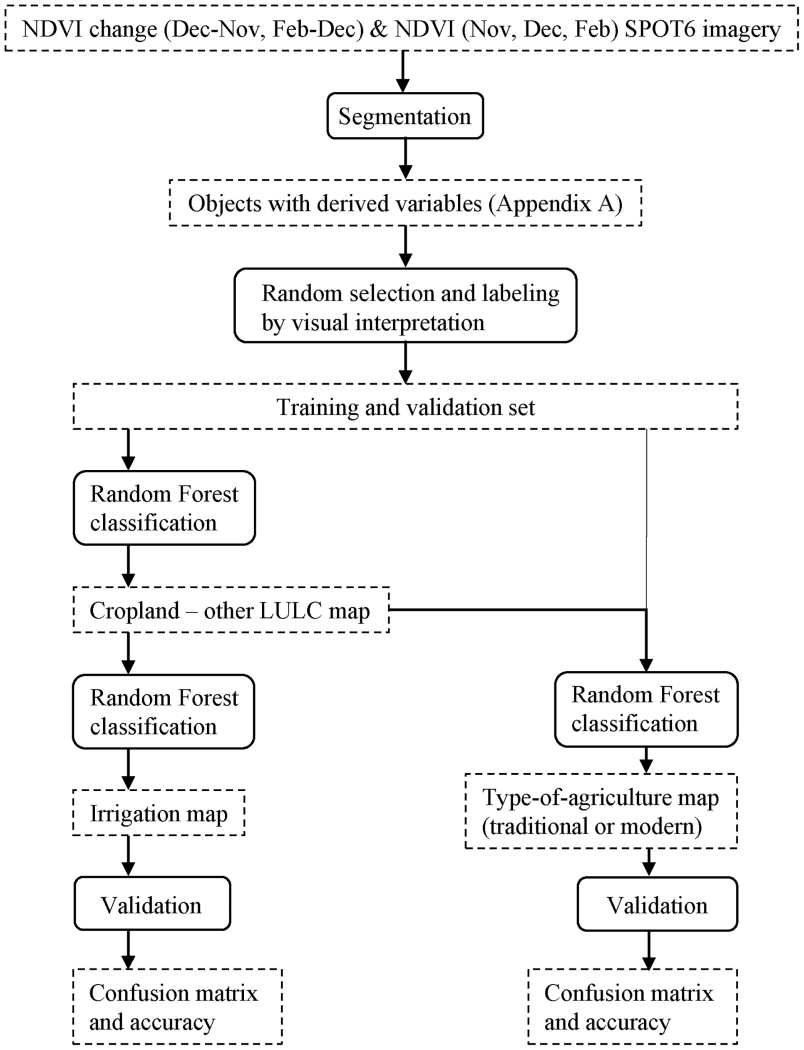

Fig. 2. Flow diagram of the GEOBIA approach of mapping irrigated agriculture and type of agriculture.

increasingly used in land-cover classifications of multi-spectral and hyper-spectral satellite imagery (Rodriguez-Galiano et al., 2012). The advantage of a Random Forest over other classifiers is that it easily handles different data types and does not require a statistically normal distribution of the dataset. Another advantage is that the Random Forest algorithm computes variable importance showing which variables are considered important for discriminating LULC classes (Rodriguez-Galiano et al., 2012). This importance is expressed by the Mean Decrease in Accuracy, defined as the drop in accuracy when leaving out the variable (Breiman, 2001). The Random Forests in this study were created using the 'randomForest' package available in the R software environment (Liaw and Wiener, 2002; R Development Core Team, 2017). The Random Forests were created using the 1316 training objects and their 57 independent variables. Irrigated agriculture was mapped using a two-step classification. Firstly, a Random Forest was created to classify the objects as either cropland or other LULC. Secondly, the objects classified as cropland were assigned to the different irrigation periods by a second Random Forest. Additionally, a Random Forest was built to allocate cropland objects into traditional smallholder or modern large-scale agriculture. The final output consisted of two maps, one showing the spatial distribution of irrigated agriculture with the period of irrigation and the other showing the spatial distribution of smallholder and large-scale agriculture.

2.3.3. Validation and performance of the classifications

Confusion matrices were computed for the classifications using the validation set (remaining 1320 objects). Overall accuracy, producer's accuracy, user's accuracy and the kappa coefficient were calculated. These classification parameters range between 0% (no match) to 100% (complete match) and are widely used to evaluate land-use classification performances in remote sensing (Lillesand et al., 2008). Accuracy results were expressed in hectares (i.e. corrected for object size).

3. Results

3.1. Delineation of landscape objects

The segmentation resulted in 42,469 objects with a mean object size of 1.6 ha. Oversegmentation occurred in the modern large-scale fields, i.e. multiple objects arose within larger fields (Fig. 3A and B), because the segmentation parameter set was optimized to maintain the per-field characteristics of smallholder agriculture (Fig. 3C). The segmentation results show that delineation on the basis of NDVI and NDVI change produces objects that generally follow field borders (Fig. 3). In the drier areas, the field borders of traditional smallholder agriculture show the lowest contrast with their surroundings, and objects do not always follow field borders.

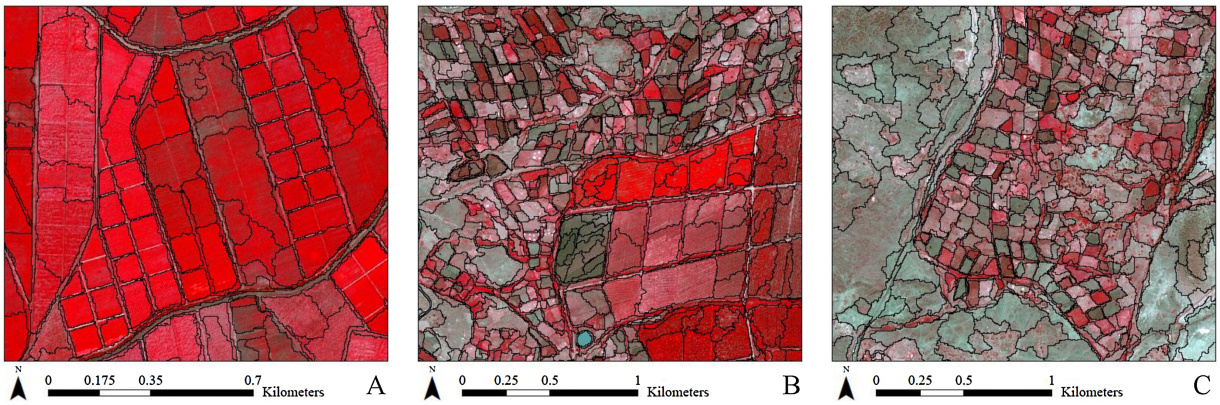

Fig. 3. Illustrations of the segmentation results on a SPOT6 image (RGB: NIR, red, green). A: Modern large-scale agriculture. B: Combination of traditional smallholder and modern large-scale agriculture agriculture. C: Traditional smallholder agriculture.

3.2. Classification of irrigated agriculture

Irrigated agriculture was mapped using a GEOBIA classification approach (Fig. 4). Overall accuracy and the kappa coefficient are 94% and 0.85 respectively (Table 1). GEOBIA shows high user's accuracies for every class with an average of 90.6% (range is 84–95%). The producer's accuracies are lower; on average 84.2% (range is 62–98%). 141 km^2 was mapped to have received irrigation water in either or both the first and second period as opposed to 52 km^2 of cropland, which received no irrigation in this time frame. Confusion is strongest between non-irrigated cropland and other LULC. Confusion is also present between other LULC and irrigated cropland p1 & p2. Objects of over-segmented fields were generally classified as a single class, hence, GEOBIA was able to identify irrigated agriculture at field level.

3.3. Mapping traditional smallholder and modern large-scale agriculture using GEOBIA

In this classification, 120 km^2 was classified as modern large-scale agriculture and 70 km^2 as traditional smallholder agriculture (Fig. 5). The overall accuracy and kappa coefficient are 95% and 0.88 respectively with high accuracy values for both types of agriculture (Table 2). Modern large-scale agriculture mostly consists of irrigated cropland p1 & p2 (Table 3). It also has a much higher classified area in irrigated cropland p1 compared to traditional smallholder agriculture. The types of agriculture have a more equal distribution for irrigated cropland p2. Traditional smallholder agriculture mostly consists of non-irrigated cropland. Generally, modern large-scale agriculture can be found in two distinct clumped areas (northeast and southwest) close to the Awash River. Traditional smallholder agriculture does not necessarily

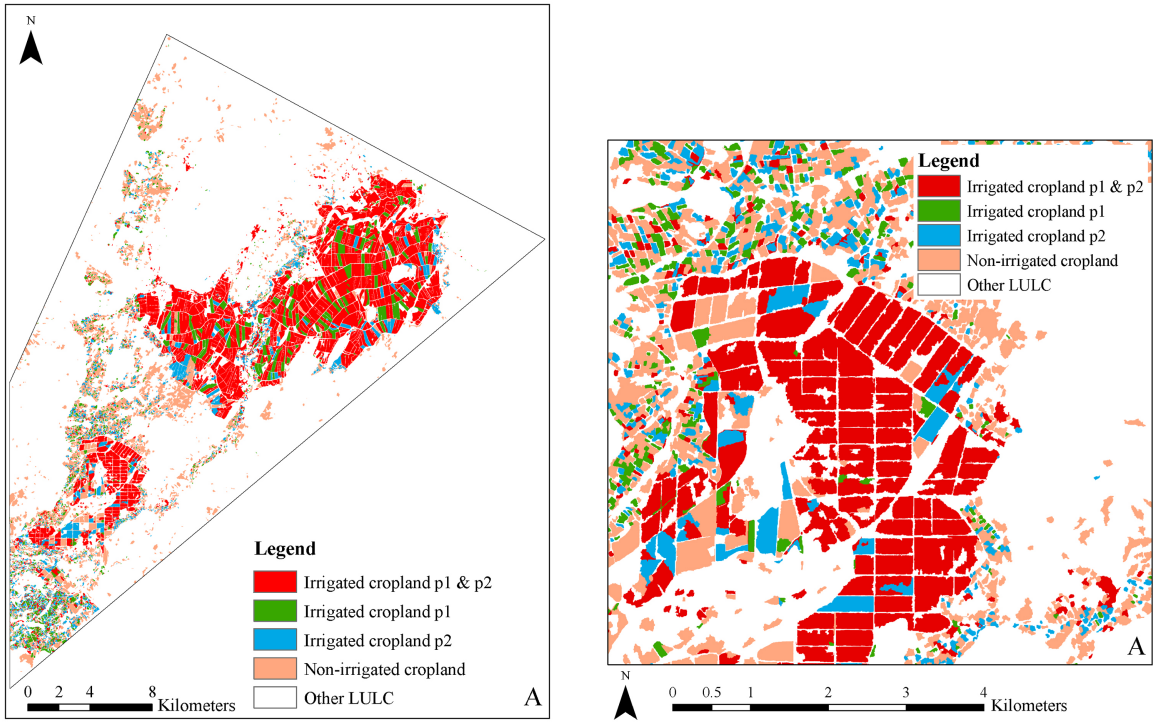

Fig. 4. A: Classification of irrigated agriculture using GEOBIA and B: Subset of this classification for a close-up illustration.

Table 1
Confusion matrix (in hectares) and accuracy for the GEOBIA classification of irrigated agriculture. Abbreviations: irr. cl. is irrigated cropland, acc. is accuracy, coef. is coefficient.

Confusion matrix	Observed							
Predicted	Irr. cl. p1 & p2	Irr. cl. p1	Irr. cl. p2	Non-Irr. cl.	Other LULC	User's acc. (%)	Mean object size (m^2)	Total mapped area (km^2)
Irr. cl. p1 & p2	296	2	2	0	17	94	12878	96
Irr. cl. p1	0	53	0	2	3	92	8062	24
Irr. cl. p2	7	0	56	0	1	88	6383	21
Non-Irr. cl.	0	12	1	145	15	84	9651	52
Other LULC	17	4	2	88	2312	95	20721	486
Producer's acc. (%)	92	76	93	62	98			
Overall acc. (%)	94							
Kappa coef.	0.85							

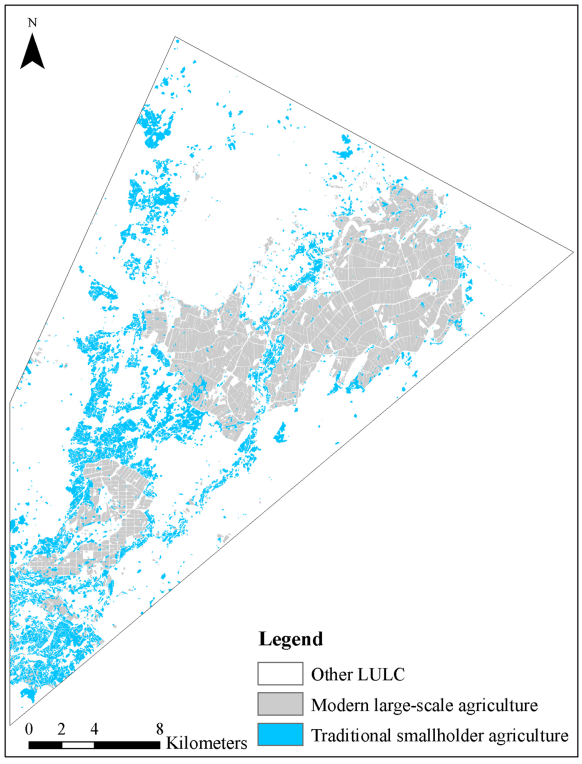

Fig. 5. Classification of traditional smallholder agriculture and modern large-scale agriculture using a GEOBIA approach.

concentrate alongside the Awash River, since most of its mapped area is non-irrigated cropland. The mean object size of modern large-scale agriculture is 2.7 times the size of the mean object size of traditional smallholder agriculture. Note that this is not equal to the average difference in field size as fields can consist of multiple objects as a result of the segmentation.

As expected, irrigation leads to high or increased NDVI values, while the values decrease when irrigation is absent (Fig. 6). Irrigated cropland p1 and irrigated cropland p2 show an increase in NDVI for their respective periods. Continuously irrigated crops show a slight decrease in NDVI in the second period, however, the NDVI is continously high and shows little variation over time. The non-irrigated cropland class is characterized by a decrease in NDVI over time. The other LULC class shows a less sharp decline in NDVI over time, which can be expected because healthy natural vegetation is also incorporated in other LULC. For non-irrigated cropland, the difference between modern large-scale agriculture (steep decline) and traditional smallholder agriculture (gentle decline) is pronounced. This gentle decline for traditional smallholder agriculture is probably related to reduced soil–water availability for the growing crop or weeds covering the field after harvest. In modern large-scale agriculture, the crop often has been harvested and the field is plowed showing bare soil or mulch.

Table 3
Mapped area and mean object size per (irrigated) agricultural class for traditional smallholder and modern large-scale agriculture. Abbreviations: irr. cl. is irrigated cropland.

Class	Type	Mapped area (km^2)	Mean object size (m^2)
Irr. cl. p1 & p2	Traditional	6	4623
	Modern	89	14,780
Irr. cl. p1	Traditional	8	4478
	Modern	15	14,083
Irr. cl. p2	Traditional	12	4554
	Modern	9	13,299
Non-Irr. cl.	Traditional	44	8946
	Modern	7	18,269

Table 2
Confusion matrix (in hectares) and accuracy for the GEOBIA classification of type of agricultural system; traditional smallholder and modern large-scale agriculture. Abbreviations: acc. is accuracy, coef. is coefficient.

Confusion matrix	Observed		
Predicted	Traditional smallholder agriculture	Modern large-scale agriculture	User's acc. (%)
Traditional smallholder agriculture	354	12	97
Modern large-scale agriculture	19	189	91
Producer's acc. (%)	95	94	
Overall acc. (%)	95		
Kappa coef.	0.88		

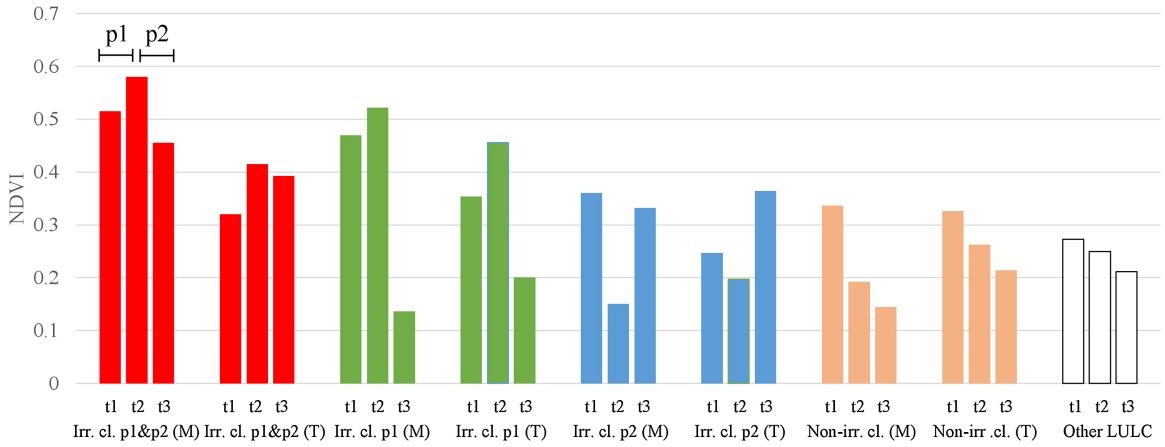

Fig. 6. NDVI over time per class. On the *Y*-axis average NDVI derived from the objects. Abbreviations: M is modern large-scale agriculture, T is traditional smallholder agriculture, t1 is Nov, t2 is Dec, t3 is Feb.

Table 4
Top 10 variable importance, ranging from 1 (most important) to 10 (less important). They are categorized by type of variable: spectral (★), shape (◁), texture (⊖), neighbour (•), location (◦). Abbreviations: ch. is change, GLCM is gray-level co-occurrence matrix (Haralick et al., 1973), corr. is correlation, con. is contrast, DN is difference to neighbours, ang. is angular second momentum, ent. is entropy, hom. is homogeneity. For complete overview of variable importance in the Random Forests and associated importance values see Appendix B.

Importance	Cropland – other LULC	Irrigation period	Modern or traditional agriculture
1.	★ Mean NDVI ch. p1	★ Mean NDVI Feb	⊖ GLCM ang. NDVI ch. p2
2.	◁ Shape index	★ Mean NDVI ch. p2	⊖ GLCM ent. NDVI ch. p2
3.	◁ Border index	★ Mean NDVI Dec	◦ X-location
4.	★ Mean NDVI ch. p2	★ Mean red Feb	⊖ GLCM ent. NDVI ch. p1
5.	★ Mean NDVI Feb	★ Mean NDVI ch. p2	⊖ GLCM ang. NDVI ch. p1
6.	⊖ GLCM corr. NDVI ch. p2	★ Mean NIR Dec	◁ Border length
7.	★ Mean NDVI Dec	★ Mean blue 1 Feb	⊖ GLCM hom. NDVI ch. p2
8.	⊖ GLCM corr. NDVI ch. p1	• Mean DN NDVI ch. p2	★ Mean red Feb
9.	★ Mean red Feb	★ Mean red Dec	★ Mean blue Feb
10.	⊖ GLCM con. NDVI ch. p2	★ Mean NIR Feb	◁ Area

3.4. Variable importance in the Random-Forest classifications

The Random Forest used 57 variables, which vary in importance for the classification process (Table 4 and Appendix B). The discrimination between cropland and other LULC is driven by a mix of spectral, shape and texture variables. Classification of the period of irrigation relies heavily on spectral variables and to a lesser extent on neighbour variables. The NDVI change appears to be important for the identification of cropland as well as determining the period of irrigation. The identification of the type of agriculture relies heavily on texture, shape and location, i.e. object features describing non-spectral characteristics allow for the distinction of type of agricultural system.

4. Discussion

GEOBIA studies successfully identified agricultural cropland area in smallholder-dominated complex landscapes (Wickama et al., 2015; Lebourgeois et al., 2017; McCarty et al., 2017; Neigh et al., 2018). This study expands on that by identifying irrigated agriculture using a GEOBIA approach as irrigated croplands have characteristic information contained in shape, texture, neighbour and location variables in addition to spectral behaviour. The results show that shape and texture information were essential for the identification of croplands. Spectral information was then dominantly used to identify the period of irrigation.

Ideally, the optimal parameter setting is the setting where over- and undersegmentation are balanced (Möller et al., 2007). It was not possible to delineate both the traditional smallholder and modern large-scale fields exactly at their field borders. Oversegmentation generally occurred in the larger fields, which allowed for the mapping of within-field variation. However, these fields were generally classified as a single class per field. Confusion occurred between other LULC and non-irrigated cropland. A large part of the other LULC in the area is relatively bare with sparse vegetation, which is spectrally similar to non-irrigated crops. The confusion between other LULC and irrigated cropland p1 & p2 is a result of the spectral similarities between a constantly irrigated cropland plot and continuously green natural vegetation. The segmentation of the images into objects using NDVI and NDVI-change information and subsequent classification showed that changes in crops occurred at field level. This illustrates that by means of the segmentation using NDVI and NVDI change, GEOBIA is able to grasp irrigated agriculture at its management level, which is important as policy and management is developed and applied at the field level. Overall, high accuracy statistics were achieved following this procedure, which illustrates its potential for monitoring the spatio-temporal patterns of irrigation scheduling for agriculture in these complex landscapes.

Agricultural policy makers focus on the identification of existing smallholder irrigation (potential), which is often clouded by the misconception that smallholder irrigation does not exist and should be developed (Beekman et al., 2014). GEOBIA proved to be able to distinguish the smallholder fields and to determine whether they are irrigated, thus have access to water resources. A combination of shape, texture, location and spectral variables was necessary to make that distinction. Interestingly, the area of an object (size of the field) is not the single-most important variable for the discrimination of type of agriculture, which might be related to the oversegmentation of the modern large-scale fields. Location in the landscape is another important variable as the different agricultural types tend to cluster in the landscape rather than appear scattered across the landscape. Texture is

the most important variable, which is likely related to the intercropping or mixed cropping systems in smallholder agriculture versus the monocropping system generally in place in modern large-scale agriculture. Although, these differences in management are also reflected in spectral variables, they are insufficient for the distinction of smallholder versus modern large-scale agriculture. The identification of smallholder agriculture is useful for monitoring the benefits or failures of irrigation investments. In general, irrigation schemes administered by smallholder farms in Ethiopia are poorly managed, and irrigation water is used inefficiently due to a lack of understanding of on-farm water management (Derib et al., 2011; Van Halsema et al., 2011). Over-irrigation is a commonly occurring phenomenon, which leads to conflicts in water-stressed areas downstream (Haileslassie et al., 2016). The GEOBIA approach presented here illustrates that the where and when of irrigation in both modern large-scale and smallholder agricultural areas can be identified and monitored at the field level.

This study showed high potential of a GEOBIA approach to map irrigated agriculture in a complex landscape in Ethiopia. The environmental settings of many other (irrigated) agricultural areas in the world show similar complexity and are a challenge for remote-sensing applications (Asgarian et al., 2016; Jin et al., 2016). Irrigation mapping methods are not easily transferable to other locations and climates, because the spectral signatures of irrigated agriculture differ and are not necessarily unique (Ozdogan et al., 2010). In general, the effect of irrigation on a field has a positive impact on crop growth, showing a change throughout the field. Also, irrigated fields are generally in the vicinity of other irrigated fields. This GEOBIA approach shows that the combination of spectral and structural parameters yields valuable information to map irrigated agriculture. The signature, expressed in spectral change, shape, texture, neighbour and location variables, is characteristic for irrigated agriculture, and hence the transferability of the method to other regions is more straightforward compared to a classification only on pixel-based spectral behavior. This study does not require ground truth acquired in the field, as the training and validation data can be created from the imagery, which makes the method easily portable to other remote regions. This is especially valuable for data-poor regions in the developing world, where policy makers and water managers are frustrated by the absence of information on actual irrigation-water applications (Droogers et al., 2010). Also, future developments in publicly-available remote sensing products (e.g. Sentinel-2) are promising for these regions. The mean object size for smallholder croplands in this study is equivalent to 46 Sentinel-2 pixels as opposed to 5 Landsat pixels, which also makes ground-truthing from this finer imagery more appealing. The 5-day revisit time of Sentinel-2 also enhances the ability to capture the temporal dynamics of irrigated agriculture, which as shown in this study, varies considerably. The spatio-temporal resolution will increasingly match the complexity of the landscapes in these settings enabling the continuous monitoring of smallholder irrigated agriculture.

5. Conclusions

This study presents a GEOBIA approach in mapping irrigated agriculture in complex landscapes. The segmentation of NDVI and NDVI-change maps produced image objects matching individual agricultural fields. Results show that it is possible to map irrigated agriculture and irrigation period with an accuracy of 94% using a GEOBIA approach with high values for the kappa coefficient (0.84), producer's (62–98%) and user's accuracy (84–95%). Spectral, shape, texture and neighbour variables are essential in the classification of irrigated agriculture. Furthermore, GEOBIA allowed for the characterization of the agricultural system, i.e. traditional smallholder farming versus modern large-scale agriculture, with an overall accuracy of 95% using spectral, shape, texture and location variables.

This method is a valuable tool in assessing the spatio-temporal dynamics of irrigated agriculture in complex landscapes, especially with the increased attention on food security and water availability in the developing world. It will help to identify areas of sub-optimal irrigation schemes and can form a basis to optimize water use for crops in smallholder irrigation and large-scale irrigation schemes.

Acknowledgements

This study is funded by Climate-KIC (Task ID: ARED0004_2013-1.1-008_P001-06).

Appendix A. Overview of variables in the GEOBIA workflow. For a detailed description see Trimble (2017)

Type	Variable	Definition
Shape	Area	The number of pixels within an object. A proxy for size.
	Border index	The smallest rectangle enclosing the object.
	Border length	Sum of the edges of the object.
	Compactness	The product of the maximum length and width divided by the number of pixels of the object.
	Length width ratio	The maximum length divided by the maximum width of the object.
	Rectangular fit	How much the object approaches the shape of a rectangle.
	Roundness	Difference between the radius of the largest enclosing ellipse and the radius of the smallest enclosing ellipse.
	Shape index	The border length of an object divided by four times the square root of its area.
Texture	GLCM angular 2^{nd} momentum NDVI (ch. p1 & p2)	Gray level co-occurrence matrix (Haralick et al., 1973).
	GLCM contrast NDVI (ch. p1 & p2), NIR (Nov, Dec, Feb)	
	GLCM correlation NDVI (ch. p1 & p2)	
	GLCM dissimilarity NDVI (ch. p1 & p2)	
	GLCM entropy NDVI (ch. p1 & p2)	
	GLCM homogeneity NDVI (ch. p1 & p2), NIR (Nov, Dec, Feb)	
	GLCM mean NDVI (ch. p1 & p2)	
	GLCM standard deviation NDVI (ch. p1 & p2)	
Spectral	Mean NDVI (ch. p1, ch. p2, Nov, Dec, Feb)	Mean NDVI value of an object.

	Mean blue (Nov, Dec, Feb)	Mean blue reflection value of an object.
	Mean green (Nov, Dec, Feb)	Mean green reflection value of an object.
	Mean red (Nov, Dec, Feb)	Mean red reflection value of an object.
	Mean NIR (Nov, Dec, Feb)	Mean near-infrared reflection value of an object.
Neighbour	Mean difference to neighbouring NDVI (ch. p1 & p2)	Weighted (with regard to length of the border between objects) layer mean difference with neighbouring objects.
	Mean difference to darker neighbouring NDVI (Nov, Dec, Feb)	Weighted (with regard to length of the border between objects) layer mean difference with neighbouring objects, which have a lower layer mean value than the object under consideration.
	Mean difference to brighter neighbouring NDVI (Nov, Dec, Feb)	Weighted (with regard to length of the border between objects) layer mean difference with neighbouring objects, which have a higher layer mean value than the object under consideration.
Location	X- and Y-location	Coordinates of the object center

Appendix B. Variable importances (Mean Decrease Accuracy) of the Random Forests

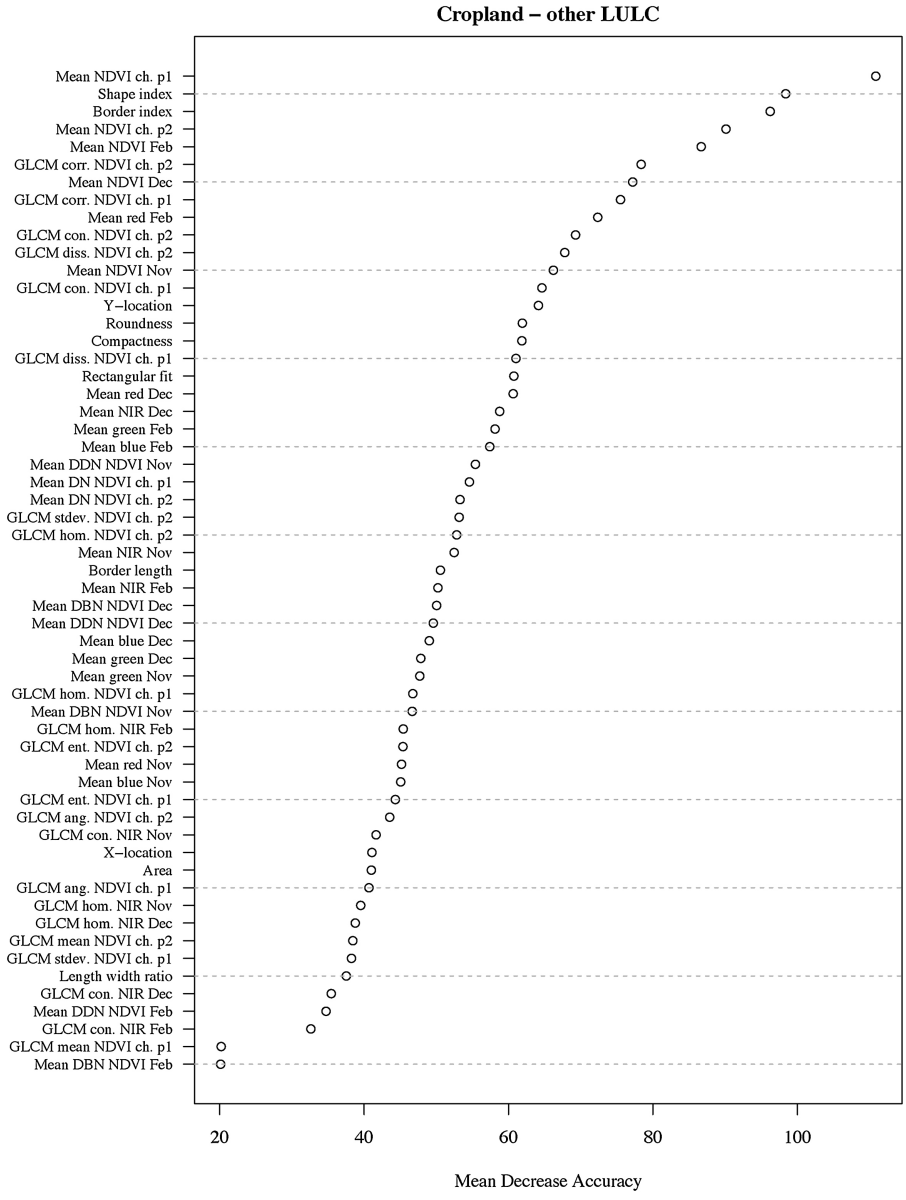

Fig. B.7. Variable importance (Mean Decrease Accuracy) of the Random Forest classifying cropland and other LULC. Abbreviations: ch. is change, p1 is period between 8 November 2013 and 4 December 2013, p2 is period between 4 December 2013 and 1 February 2014, GLCM is gray-level co-occurrence matrix, ang. is angular 2^{nd} momentum, con. is contrast, corr. is correlation, diss. is dissimilarity, ent. is entropy, hom. is homogeneity, stdev. is standard deviation, DN is difference to neighbours, DDN is difference to darker to neighbours, DBN is difference to brighter neighbours.

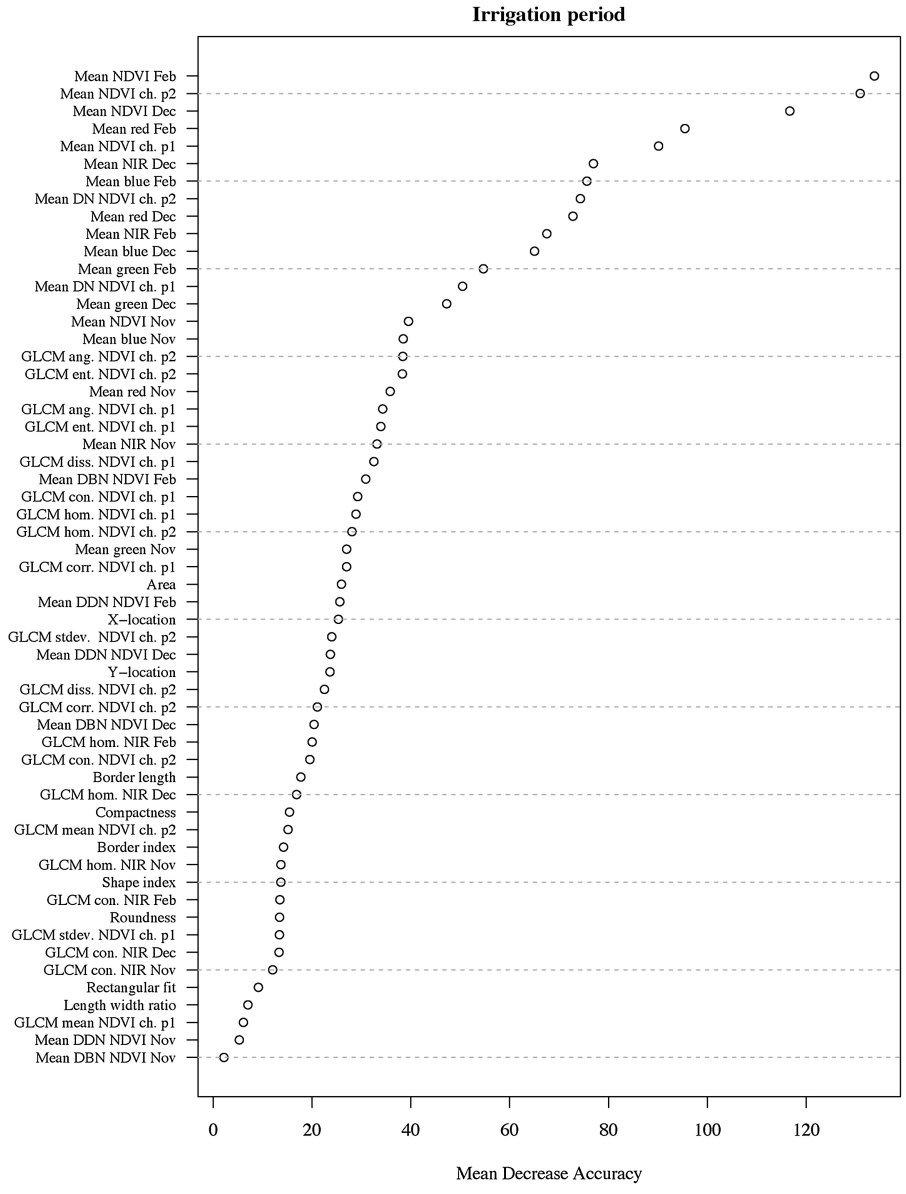

Fig. B.8. Variable importance (Mean Decrease Accuracy) of the Random Forest classifying irrigation period. Abbreviations: ch. is change, p1 is period between 8 November 2013 and 4 December 2013, p2 is period between 4 December 2013 and 1 February 2014, GLCM is gray-level co-occurrence matrix, ang. is angular 2^{nd} momentum, con. is contrast, corr. is correlation, diss. is dissimilarity, ent. is entropy, hom. is homogeneity, stdev. is standard deviation, DN is difference to neighbours, DDN is difference to darker to neighbours, DBN is difference to brighter neighbours.

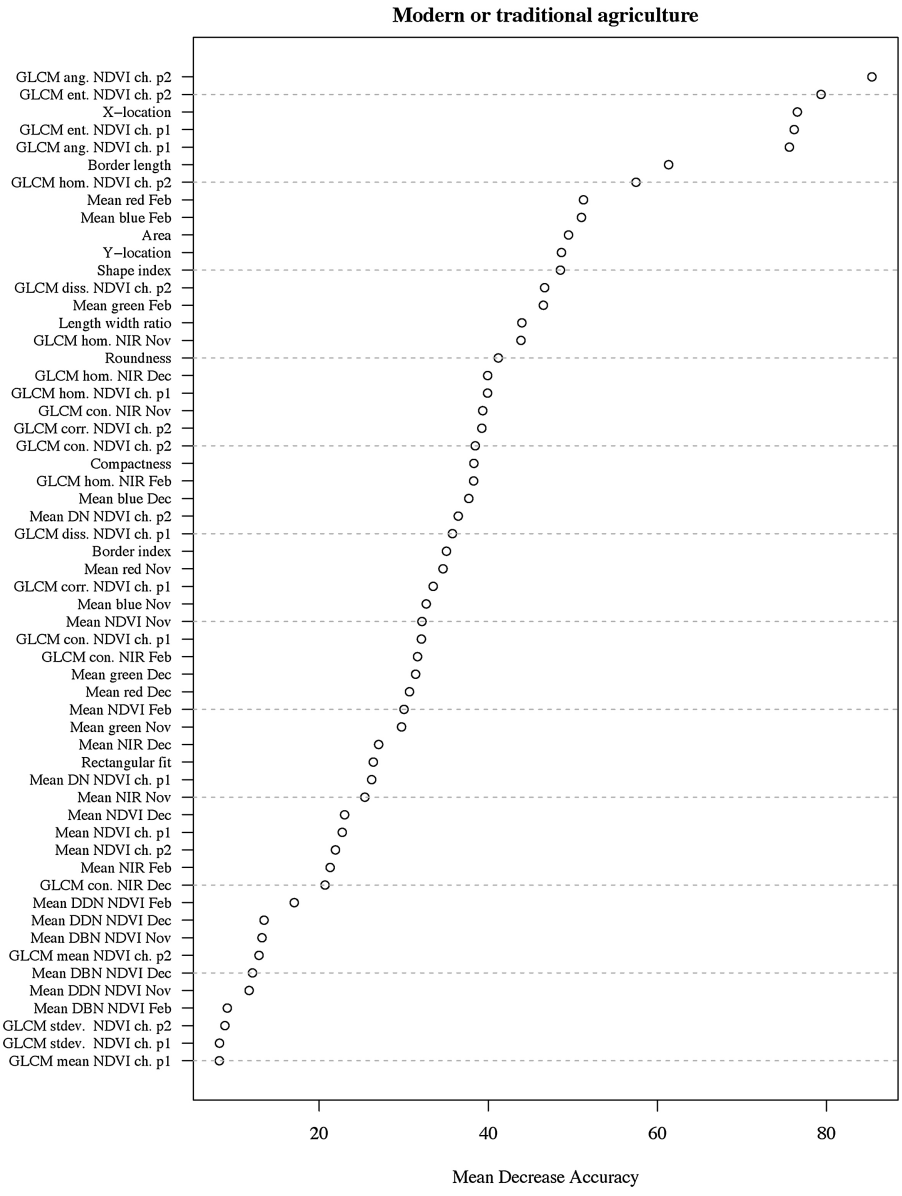

Fig. B.9. Variable importance (Mean Decrease Accuracy) of the Random Forest classifying modern large-scale and traditional smallholder agriculture. Abbreviations: ch. is change, p1 is period between 8 November 2013 and 4 December 2013, p2 is period between 4 December 2013 and 1 February 2014, GLCM is gray-level co-occurrence matrix, ang. is angular 2^{nd} momentum, con. is contrast, corr. is correlation, diss. is dissimilarity, ent. is entropy, hom. is homogeneity, stdev. is standard deviation, DN is difference to neighbours, DDN is difference to darker to neighbours, DBN is difference to brighter neighbours.

References

Abate, T., Van Huis, A., Ampofo, J., 2000. Pest management strategies in traditional agriculture: an African perspective. Annu. Rev. Entomol. 45, 631–659.

Abuzar, M., McAllister, A., Whitfield, D., 2015. Mapping irrigated farmlands using vegetation and thermal thresholds derived from Landsat and ASTER data in an irrigation district of Australia. Photogramm. Eng. Remote Sens. 81, 229–238.

Ambika, A., Wardlow, B., Mishra, V., 2016. Remotely sensed high resolution irrigated area mapping in India for 2000 to 2015. Sci. Data 3, 1–14.

Asgarian, A., Soffianian, A., Pourmanafi, S., 2016. Crop type mapping in a highly fragmented and heterogeneous agricultural landscape: a case of central Iran using multi-temporal Landsat 8 imagery. Comput. Electron. Agric. 127, 531–540.

Baatz, M., Schäpe, A., 2000. Multiresolution segmentation: an optimization approach for high quality multi-scale image segmentation. Angew. Geogr. Info. verarbeitung, Wichmann-Verlag, Heidelberg 12–23.

Beekman, W., Veldwisch, G., Bolding, A., 2014. Identifying the potential for irrigation development in Mozambique: capitalizing on the drivers behind farmer-led irrigation expansion. Phys. Chem. Earth Parts A/B/C 76-78, 54–63.

Beilicci, E., Beilicci, R., 2016. Irrigation influence on catchment hydrology modelling with advanced hydroinformatic tools. Res. J. Agric. Sci. 48, 10–21.

Benz, U.C., Hofmann, P., Willhauck, G., Lingenfelder, I., Heynen, M., 2004. Multi-resolution, object-oriented fuzzy analysis of remote sensing data for GIS-ready information. ISPRS J. Photogramm. Remote Sens. 58, 239–258.

Blaschke, T., Hay, G.J., Kelly, M., Lang, S., Hofmann, P., Addink, E., Queiroz Feitosa, R., Van der Meer, F., Van der Werff, H., Van Coillie, F., Tiede, D., 2014. Geographic object-based image analysis – towards a new paradigm. ISPRS J. Photogramm. Remote Sens. 87, 180–191.

Breiman, L., 2001. Random forests. Mach. Learn. 45, 5–32.

Bruinsma, J., 2009. The resource outlook to 2050: by how much do land, water and crop yields need to increase by 2050? Tech. Rep Prepared for the FAO expert meeting on 'How to feed the world in 2050', Rome.

Burney, J.A., Naylor, R.L., 2012. Smallholder irrigation as a poverty alleviation tool in sub-Saharan Africa. World Dev. 40, 110–123.

Conrad, C., Fritsch, S., Zeidler, J., Rücker, G., Dech, F., 2010. Per-field irrigated crop classification in arid Central Asia using SPOT and ASTER data. Remote Sens. 2, 1035–1056.

Dejen, Z.A., 2014. Hydraulic and Operational Performance of Irrigation System in View of Interventions for Water Saving and Sustainability. Ph.D. Thesis. UNESCO-IHE Institute for Water Education, Delft.

Derib, S.D., Descheemaeker, K., Haileslassie, A., Amede, T., 2011. Irrigation Water Productivity as Affected by Water Management in a Small-Scale Irrigation Scheme in the Blue Nile Basin, Ethiopia. Exp. Agric. 47, 39–55.

Droogers, P., Aerts, J., 2005. Adaptation strategies to climate change and climate

variability: a comparative study between seven contrasting river basins. Phys. Chem. Earth 30, 339–346.
Droogers, P., Immerzeel, W.W., Lorite, I.J., 2010. Estimating actual irrigation application by remotely sensed evapotranspiration observations. Agric. Water Manag. 97, 1351–1359.
ESRI, 2017. ArcGIS Online Standard Service: World Imagery Collection, Map Server. Maps Throughout This Book Were Created Using ArcGIS® Software by ESRI. ArcGIS® and ArcMapTM are the Intellectual Property of ESRI and are Used Herein Under License, Copyright©ESRI. For More Information About ESRI® Software. and http://www.esri.com (accessed 29.11.17). http://www.services.arcgisonline.com/ArcGIS/rest/services/WorldImagery/MapServer.
FAO, 2010. FAO Crop Calender. (accessed 14.11.17). http://www.fao.org/agriculture/seed/cropcalendar/cropcal.do.
FAO, 2011. The State of the World's Land and Water Resources for Food and Agriculture (SOLAW) – Managing Systems at Risk. Food and Agriculture Organization of the United Nations, Rome and Earthscan, London.
Google Maps. (accessed 29.11.17). https://www.google.nl/maps/place/Metehara.
Haileslassie, A., Agide, Z., Erkossa, T., Hoekstra, D., Schmitter, P., Langan, S., 2016. On-Farm Smallholder Irrigation Performance in Ethiopia: From Water Use Efficiency to Equity and Sustainability. LIVES Working Paper 19: International Livestock Research Institute, Nairobi, Kenya.
Haralick, R.M., Shanmugam, K., Dinstein, I., 1973. Textural features for image classification. IEEE Trans. Syst. Man Cybern. 3, 610–621.
IAC, 2004. Realizing the Promise and Potential of African Agriculture: Implementation of Recommendations and Action Agenda. InterAcademy Council, Amserdam, The Netherlands.
Jin, N., Tao, B., Ren, W., Feng, M., Sun, R., He, L., Zhuang, W., Yu, Q., 2016. Mapping irrigated and rainfed wheat areas using multi-temporal satellite data. Remote Sens. 8, 1–19.
Lebourgeois, V., Dupuy, S., Vintrou, É., Ameline, M., Butler, S., Bégué, A., 2017. A combined random forest and OBIA classification scheme for mapping smallholder agriculture at different nomenclature levels using multisource data (simulated Sentinel-2 time series, VHRS and DEM). Remote Sens. 9, 1–20.
Liaw, A., Wiener, M., 2002. Classification and regression by randomForest. R News 2, 18–22.
Lillesand, T., Kiefer, R., Chipman, J., 2008. Remote Sensing and Image Interpretation, 6th ed. John Wiley & Sons, New York.
McCarty, J., Neigh, C., Carroll, M., Wooten, M., 2017. Extracting smallholder cropped area in Tigray, Ethiopia with wall-to-wall sub-meter WorldView and moderate resolution Landsat 8 imagery. Remote Sens. Environ. 202, 142–151.
Meier, J., Zabel, F., Mauser, W., 2018. A global approach to estimate irrigated areas – a comparison between different data and statistics. Hydrol. Earth Syst. Sci. 22, 1119–1133.
Möller, M., Lymburner, L., Volk, M., 2007. The comparison index: a tool for assessing the accuracy of image segmentation. Int. J. Appl. Earth Observ. Geoinf. 9, 311–321.
Neigh, C., Carroll, M., Wooten, M., McCarty, J., Powell, B., Husak, G., Enenkel, M., Hain, C., 2018. Smallholder crop area mapped with wall-to-wall WorldView sub-meter panchromatic image texture: a test case for Tigray, Ethiopia. Remote Sens. Environ. 212, 8–20.
Ozdogan, M., Yang, Y., Allez, G., Cervantes, C., 2010. Remote sensing of irrigated agriculture: opportunities and challenges. Remote Sens. 2, 2274–2304.
Peña, J., Gutiérrez, P., Hervás-Martínez, C., Six, J., Plant, R., López-Granados, F., 2014. Object-based image classification of summer crops with machine learning methods. Remote Sens. 6, 5019–5041.
R Development Core Team, 2017. R: A Language and Environment for Statistical Computing. R Foundation for Statistical Computing, Vienna, Austria.
Rodriguez-Galiano, V.F., Ghimire, B., Rogan, J., Chica-Olmo, M., Rigol-Sanchez, J.P., 2012. An assessment of the effectiveness of a random forest classifier for land-cover classification. ISPRS J. Photogramm. Remote Sens. 67, 93–104.
Siddiqui, S., Cai, X., Chandrasekharan, K., 2016. Irrigated Area Map Asia and Africa (International Water Management Institute). http://waterdata.iwmi.org/applications/irri_area/.
Taddese, G., Sonder, K., Peden, D., 2010. The Water of the Awash River Basin: A Future Challenge to Ethiopia. Working paper: International Livestock Research Institute, Addis Ababa, Ethiopia.
Thenkabail, P.S., Schull, M., Turral, H., 2005. Ganges and Indus river basin land use/land cover (LULC) and irrigated area mapping using continuous streams of MODIS data. Remote Sens. Environ. 95, 317–341.
Thiruvengadachari, S., 1981. Satellite sensing of irrigation patterns in semiarid areas: an Indian study. Photogramm. Eng. Remote Sens. (USA) 47, 1493–1499.
Trimble, 2017. eCognition Developer 9.3 Reference Book, Trimble Germany Documentation, München, Germany.
Tschirley, D., 2011. What is the Scope for Horticulture to Drive Smallholder Poverty Reduction in Africa? Policy Synthesis, vol. 88 USAID, University of Michigan.
USGS, 2016a. 1. Some Irrigation Methods. (accessed 14.11.17). https://water.usgs.gov/edu/irquicklook.html.
USGS, 2016b. 2. Irrigation Water Use: Surface Irrigation. (accessed 14.11.17). https://water.usgs.gov/edu/irfurrow.html.
Van Halsema, G.E., Keddi Lencha, B., Assefa, M., Hengsdijk, H., Wesseler, J., 2011. Performance assessment of smallholder irrigation in the central rift valley of Ethiopia. Irrig. Drain. 60, 622–634.
Vorosmarty, C.J., Sahagain, D., 2000. Anthropogenic disturbance of the terrestrial water cycle. BioScience 50, 753–765.
Wickama, J., Masselink, R., Sterk, G., 2015. The effectiveness of soil conservation measures at a landscape scale in the West Usambara highlands, Tanzania. Geoderma 241–242, 168–179.
World Bank, 2008. World Development Report 2008: Agriculture for Development. Washington D.C., USA.
WWAP, 2012. World Water Assessment Programme. The United Nations World Water Development Report 4: Managing Water Under Uncertainty and Risk.
Xie, H., You, L., Wielgosz, B., Ringler, C., 2014. Estimating the potential for expanding smallholder irrigation in Sub-Saharan Africa. Agric. Water Manag. 131, 183–193.
You, L., Ringler, C., Wood-Sichra, U., Robertson, R., Wood, S., Zhu, T., Nelson, G., Guo, Z., Sun, Y., 2011. What is the irrigation potential for Africa? A combined biophysical and socioeconomic approach. Food Policy 36, 770–782.